Graphene Photodetector Based on Metamaterial Perfect Absorber

Shichao Song[1], **Long Wen**[1], and **Qin Chen**[1,2]

[1]Key Lab of Nanodevices and Applications-CAS
Collaborative Innovation Center of Suzhou Nano Science and Technology
Suzhou Institute of Nano-Tech and Nano-Bionics, Chinese Academy of Sciences (CAS)
Suzhou 215123, China
[2]Peking University Shenzhen SOC Key Laboratory, PKU-HKUST Shenzhen-Hong Kong Institute
Hi-Tech Industrial Park South, Shenzhen 518057, China

Abstract— A graphene-metamaterial composite photodetectors with graphene embedded in metamaterial perfect absorbers (MPAs) is proposed and their light absorption properties are numerically investigated. Absorption above 40% in graphene monolayer is obtained due to the strongly localized electromagnetic resonance and the suppression of reflection and transmission loss in MPAs. The working frequency of the graphene photodetector can be tunable and determined by MPAs due to the ultrabroad absorption band of graphene. The novel idea of using MPAs to enhance the interaction between light and graphene could be also adopted in other graphene optoelectronic devices.

1. INTRODUCTION

Graphene is an attractive material for optoelectronic devices such as transparent conductive electrode, polarization controller, modulator, photodetector, due to its ultra-broadband absorption, unusually high electron mobility, atomic layer thickness, and unique mechanical flexibility [1]. With a thickness of only 0.335 nm, monolayer graphene exhibits remarkable optical absorption nearly 2.3% in a wide frequency range from ultraviolet to infrared [2]. However, monolayer or few layer graphene has very weak light absorption due to the sub-1 nm-scale thickness, resulting in very low photoresponsivity, especially in graphene photodetectors. An ultrafast transistor-based photodetector with a bandwidth of 40 GHz was demonstrated but the photoresponse was only $0.5\,\mathrm{mAW^{-1}}$ [3] Konstantatos et al. constructed a graphene-colloidal quantum dots composited nanostructure with a responsivity of $\sim 10^7\,\mathrm{AW^{-1}}$, but it is a responsivity of composited nanostructure rather than simple graphene response [4]. Various methods have been presented to improve the photoresponse by enhancing the interaction between graphene and light. Furchi et al. demonstrated a graphene photodetector based on a dielectric planar microcavity with a photoresponse of 21 $\mathrm{mAW^{-1}}$. Absorption as high as 60% was obtained but the device was quite complex due to the large number of dielectric layers in the distributed Bragg reflectors [5]. Instead, Engel et al. used metallic mirrors to form a simple microcavity but the surface reflection and the metal attenuation reduced the photoresponse [6]. Alternatively, Zhang et al. has proposed a novel idea to greatly enhance the photoresponsivity of the graphene photodetector by engineering the lifetime of the photo-excited carriers, where the graphene was patterned into quantum dot-like structures [7]. On the other hand, perfect absorption at terahertz frequency was achieved in graphene by patterning into nanodisk array and forming a metamaterial perfect absorber (MPA) [8]. In this case, doped graphene, like the noble metals in the visible and near infrared regime, supports surface plasmon resonances (SPRs). It therefore acts as surface impedance matching layer in a MPA. But for infrared and visible range, the electron density in doped graphene is not high enough to support SPRs. Meanwhile, metallic MPAs have been widely investigated and demonstrated promising applications in biosensor [9], microbolometers [10], solar cells [11, 12], etc. Usually, it consists of a structured metallic surface and a metallic ground plane intermediated by a dielectric layer [9, 13, 14]. Matching the surface impedance by optimizing the periodic subwavelength structures in the top metal film, a near-zero reflection can be achieved. The metallic ground plane acts as a perfect reflector. As a result, near-unity absorption of the whole structure is obtained at the electromagnetic resonance.

In this letter, a pair of novel graphene-material composite structures for high-efficiency photodetection is proposed, where each graphene monolayer is embedded in a MPA. The configuration of a graphene MPA naturally coincides with a transistor, where the metallic impedance matching layer and the ground plane can be used as electrodes and gate, respectively. Compared to the previous devices, it provides both high light absorption in graphene and simple device structures. Finite difference time domain (FDTD) method is used to simulate the light transmission behaviour. The electromagnetic properties of the sandwich structure are optimized to perfectly meet the impedance match condition. As a result of the high reflection back mirror and the impedance matching, a nearly unit absorption could be achieved on resonance, in which 40% incident light is absorbed in graphene, 17 times enhancement compared to graphene intrinsic absorption. Tunable absorption spectra are also demonstrated.

Schematic of a pair of graphene photodetectors with graphene embedded in MPAs are shown in Fig. 1. One dimensional (1D) metal gratings (Fig. 1(a)) or a continuous metal film with square hole arrays (Fig. 1(b)) is separated from a continuous metal film by a layer of Al_2O_3. Graphene is just at the bottom of the metal gratings. FDTD simulations of a unit cell were performed with periodic boundary conditions in the x direction or xy plane and perfect matching layers in the z direction. Non-uniform meshes were used in the FDTD simulation, where the minimum mesh sizes at the interfaces are 5 nm and 0.1 nm in horizontal and vertical directions, respectively. The incident light is assumed to be transverse magnetic (TM) polarized (the magnetic field parallel to the grating) and normal to the structure surface. The refractive index of Al_2O_3 is 1.7. Gold is used as the metal material with dielectric constant from the data of Johnson and Christ [15]. The dielectric constant of graphene is $1 + 4\pi i\sigma/\omega t$, where σ is the conductivity, ω is the angular frequency and t is the thickness of graphene (0.5 nm in the simulation) [16]. The conductivity from both interband and intraband contributions for graphene are calculated using the Kubo formula [17, 18]

$$\sigma inter(\omega) = \frac{\pi e^2}{4h}\left(\tanh\frac{\hbar\omega+2\mu}{4k_bT}+\tanh\frac{\hbar\omega-2\mu}{4k_bT}\right)+i\left(\frac{1}{\hbar\omega}\frac{2e^2}{h}\mu-\frac{e^2}{2h}\log\left|\frac{\hbar\omega+2\mu}{\hbar\omega-2\mu}\right|\right) \quad (1)$$

$$\sigma intra(\omega) = i\frac{2e^2}{h}\frac{2k_bT}{\hbar(\omega+i\tau^{-1})}\log\left(2\cosh\left(\frac{\mu}{2k_bT}\right)\right) \quad (2)$$

$$\sigma(\omega) = \sigma inter(\omega)+\sigma intra(\omega) \quad (3)$$

where σ_{intra}, σ_{inter} are the intraband and interband contribution to conductivity, respectively. h and $\hbar$ are Planck and reduced Planck constant. ω is the angular frequency, μ is the chemical potential of graphene, which can be set to 0 eV via the applied voltage. k_b is Boltzmann constant, T is the thermodynamic temperature (300 K). e is the charge of electron, τ is the average scattering lifetime of free electrons.

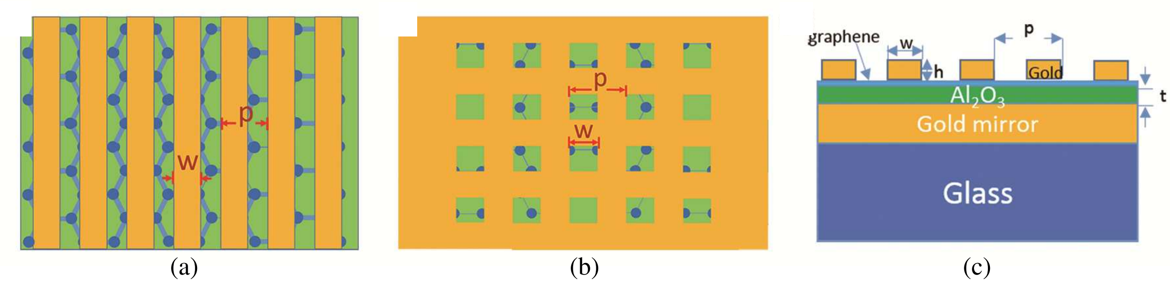

Figure 1: Schematic of a pair of graphene photodetectors with graphene embedded in MPAs. (a) Top view of a graphene photodetector. The matallic matching layer is the gold gratings. (b) Top view of metallic hole array assembled graphene photodetector. The metallic matching layer is the gold film with square hole arrays. (c) The section cross view of the first MPA structure (a).

Figure 2(a) shows the calculated absorption spectra of a whole MPA and the contribution from graphene. It can be seen that the light is nearly completely absorbed at the resonant wavelength, among which 40.1% absorption occurs in graphene. The effective permeability ($\mu' + i\mu''$) of the MPA were also calculated [19]. As presented in Fig. 2(b), μ' cross zero at 1.065 µm, which results in the impedance matching at this wavelength. Meanwhile, μ'' has a positive resonance at the corresponding wavelength. Thus, the complete absorption is mainly attributed to the occurrence of the magnetic absorption resonance. With this effect, the light absorption is enhanced by over 17 times that of an intrinsic graphene monolayer. The proposed graphene MPA photodetector can be regarded as a combination of a plasmonic photodetector and a microcavity photodetector, where both SPR near field enhancement and light path recycling contribute to the light absorption. Furthermore, the perfect impedance match at the patterned metal structure eliminates the reflection loss. The plasmonic near field enhancement can be seen from Fig. 2(e), where hot spots exist beneath the

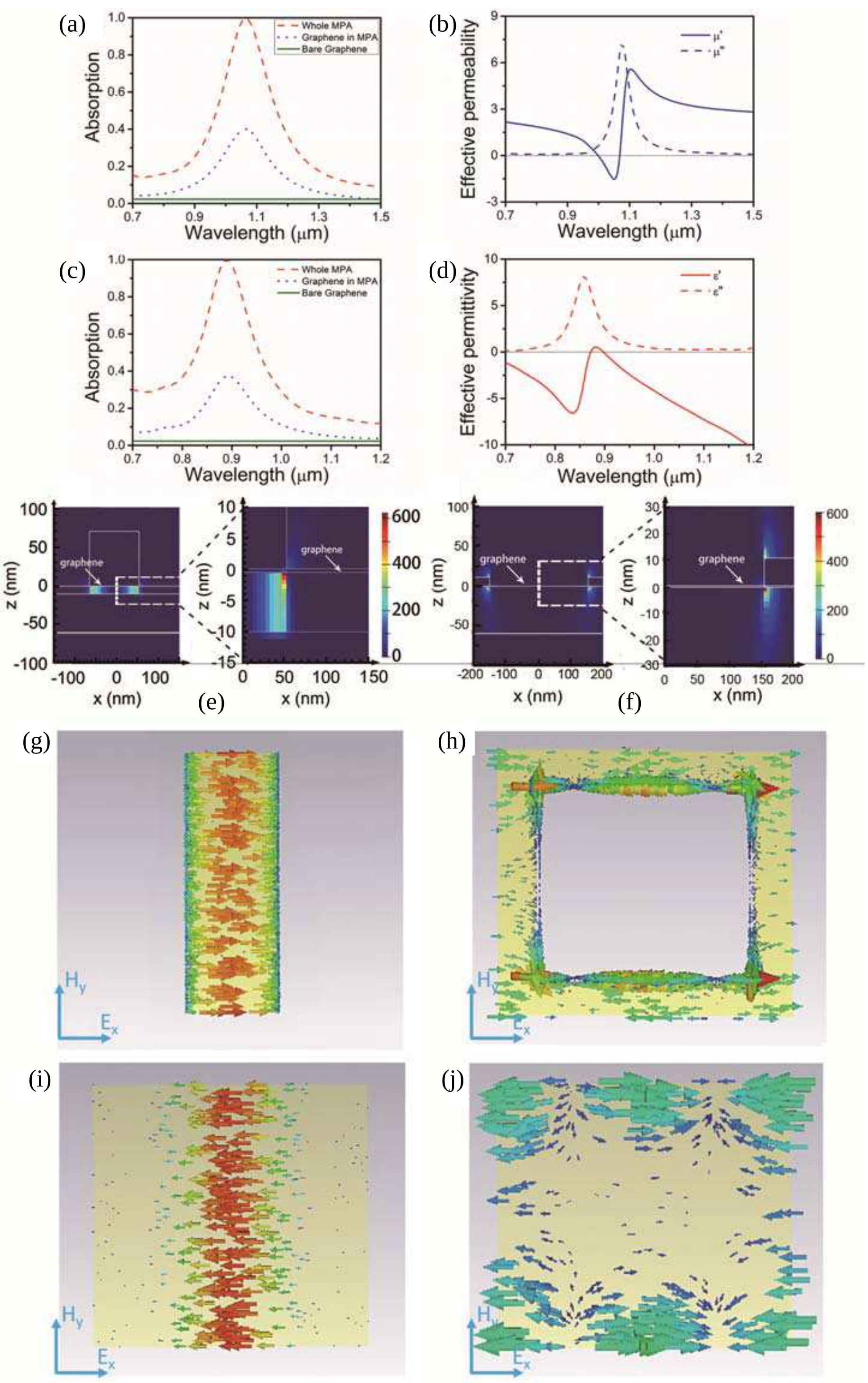

Figure 2: (a) Absorption spectrum of a graphene monolayer in MPA with the TM polarized normal incident light, with $p = 300\,\mathrm{nm}$, $w = 110\,\mathrm{nm}$, $h = 70\,\mathrm{nm}$, and $t = 10\,\mathrm{nm}$. The absorption spectra of the whole MPA and a bare graphene monolayer are shown for comparison Graphene locates at the bottom of the gratings. (b) Absorption spectrum of a graphene monolayer in MPA (shown in the Fig. 1(b), whith $p = 400\,\mathrm{nm}$, $w = 310\,\mathrm{nm}$, $h = 10\,\mathrm{nm}$, and $t = 60\,\mathrm{nm}$. (c), (d) The effective permittivity and permeability are also calculated. The distribution of $|E_z|^2$ at the resonant wavelength of (e) 1.065 μm and (f) 0.896 μm in a unit cell. The zoom-in electric field distribution around the edge of the nanostructure is also presented. The semi-transparent schematics of the induced surface currents of the MPA at each resonant wavelength with different metallic surfaces. (g) and (h) are the top view of induced surface currents of nanostructures, (i) and (j) are the induced surface currents of the metallic mirrors, respectively.

grating corners with more than 600 times enhancement of $|E_z|^2$. The excellent light trapping allows a strong interaction between graphene and light. MPA consisting of two-dimensional metallic hole array as shown in Fig. 1(b) were also investigated for the metamaterial-graphene photodetector. As shown in Fig. 2(c), the light has almost been completely absorbed at the resonant wavelength, where 37.3% absorption contribution is from graphene. The effective permittivity ($\varepsilon' + i\varepsilon''$) of the MPA are presented in the Fig. 2(d). ε' cross zero at 0.896 μm. Moreover, the imaginary part has a positive value, contributing to the light absorption. So the light absorption in graphene can be significantly enhanced by electromagnetic resonance at the resonant wavelength. The strong plasmonic near field enhancement can be seen from Fig. 2(f), where hot spots exist at the edge of the nanostructures. Owing to enhancement of $|E_z|^2$, the absorption of graphene has been largely enhanced. The schematic figures of calculated surface current of these two MPAs at each resonant wavelength are shown in Figs. 2(g)–(j), respectively. In Figs. 2(g) and (i), the induced surface currents at two metal/dielectric interfaces flow in opposite directions, generating a magnetic field opposite to the external field. This also confirms that the absorption of this MPA structure (gratings) at the resonant wavelength is donated by the magnetic resonance. While the current distribution in the hole array nanostructures are different as shown in Fig. 2(h). In each metal-dielectric interface, the surface current has opposite flow directions at different regions, for example, in Fig. 2(j), the surface currents at four corners flow from right to left while those at the top and bottom edges flow from left to right. The sum of surface current is very small resulting the suppression of the magnetic resonance. On the contrary, the dipole-like current distributions between the two corners along the direction of the excitation electric field show an electric resonance. Therefore, by constructing different subwavelength structures, we can manipulate the spectral response of the MPA based on both electric and magnetic resonances and optimize the graphene-metamaterial photodetectors.

Since the absorption enhancement results from the strong light localization in MPA and its interaction with graphene, it is necessary to investigate the effect of various structure parameters. The positions of graphene in the MPA are proved to be at the bottom of the gold gratings, contributing to the largest enhancement. Moreover, the period has little effect on the resonant wavelength and absorption, while the duty ratio of the nanostructures has a great influence on them [20]. Shown in Fig. 3(a), six graphene embedded MPAs with a same period are shown, where the absorption wavelengths are linearly tuned by the widths or fill factor of the gold gratings. The maximum light absorbance of 40.1%, approximately 17.4 times of the instinct graphene absorption, is observed at $w = 100$ nm, where the near-field enhancement approaches a maximum at the edge of the gratings. Several graphene embedded hole array MPAs with a same period are also shown in Fig. 3(b), where the absorption wavelengths are monotonously changed by the duty ratio or the side length of the hole. Moreover, over 35% absorption of graphene can be achieved in these MPAs with the near-field enhancement.

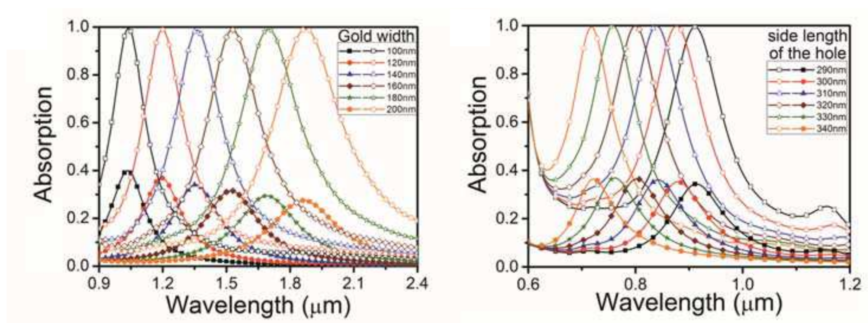

(a) (b)

Figure 3: The absorption spectra in various MPAs. Graphene is at the bottom of the gold nanostructures. (a) Whole structure (open scatters) and graphene (solid scatters) absorption spectra for $w = 100$–200 nm. $p = 300$ nm, $h = 70$ nm, $t = 10$ nm. (b) Whole structure (open scatters) and graphene (solid scatters) absorption spectra for $w = 290$–340 nm. $p = 400$ nm, $h = 10$ nm, $t = 60$ nm.

2. CONCLUSIONS

A novel graphene-metamaterial composite structure with graphene monolayer embedded in a MPA is proposed and its light absorption property is numerically investigated. Over 40% absorption in graphene is achieved, which is over 17 times that of a bare monolayer graphene. Owing to the strongly localized electromagnetic resonance and the suppression of reflection and transmission loss in MPAs, the absorption can be significantly enhanced. Benefiting from graphene's ultra-wideband optical absorption and high electron mobility, we can obtain a photodetector with high speed, broad band and high photoelectric conversion efficiency. This novel idea using MPAs to enhance the interaction between light and graphene not only presents a new solution to graphene photodetectors, but also could be adopted in other graphene optoelectronic devices.

ACKNOWLEDGMENT

This work is supported by the General Program of the National Natural Science Foundation of China (No. 11274344), the Hundred Talents Program of Chinese Academy of Sciences and the Fundamental Research Project of Shenzhen Science and Technology Foundation (No. JC201105180781A).

REFERENCES

1. Mueller, T., F. N. A. Xia, and P. Avouris, *Nat. Photonics*, Vol. 4, No. 5, 297–301, 2010.
2. Nair, R. R., P. Blake, A. N. Grigorenko, K. S. Novoselov, T. J. Booth, T. Stauber, N. M. R. Peres, and A. K. Geim, *Science*, Vol. 320, No. 5881, 1308–1308, 2008.
3. Xia, F. N., T. Mueller, Y. M. Lin, A. Valdes-Garcia, and P. Avouris, *Nat. Nanotechnol.*, Vol. 4, No. 12, 839–843, 2009.
4. Konstantatos, G., M. Badioli, L. Gaudreau, J. Osmond, M. Bernechea, F. P. G. de Arquer, F. Gatti, and F. H. L. Koppens, *Nat. Nanotechnol.*, Vol. 7, No. 6, 363–368, 2012.
5. Furchi, M., A. Urich, A. Pospischil, G. Lilley, K. Unterrainer, H. Detz, P. Klang, A. M. Andrews, W. Schrenk, G. Strasser, and T. Mueller, *Nano. Lett.*, Vol. 12, No. 6, 2773–2777, 2012.
6. Engel, M., M. Steiner, A. Lombardo, A. C. Ferrari, H. V. Löhneysen, P. Avouris, and R. Krupke, *Nat. Commun.*, Vol. 3, 906, 2012.
7. Zhang, B. Y., T. Liu, B. Meng, X. Li, G. Liang, X. Hu, and Q. J. Wang, *Nat. Commun.*, Vol. 4, 1811, 2013.
8. Thongrattanasiri, S., F. H. L. Koppens, and F. J. G. de Abajo, *Phys. Rev. Lett.*, Vol. 108, No. 4, 047401, 2012.
9. Liu, N., M. Mesch, T. Weiss, M. Hentschel, and H. Giessen, *Nano. Lett.*, Vol. 10, No. 7, 2342–2348, 2010.
10. Maier, T. and H. Bruckl, *Opt. Lett.*, Vol. 34, No. 19, 3012–3014, 2009.
11. Choi, H., F. Borondics, D. A. Siegel, S. Y. Zhou, M. C. Martin, A. Lanzara, and R. A. Kaindl, *Appl. Phys. Lett.*, Vol. 94, 172102, 2009.
12. Wen, L., F. H. Sun, and Q. Chen, *Appl. Phys. Lett.*, Vol. 104, No. 15, 151106, 2014.
13. Landy, N. I., S. Sajuyigbe, J. J. Mock, D. R. Smith, and W. J. Padilla, *Phys. Rev. Lett.*, Vol. 100, No. 20, 207402, 2008.
14. Chen, Q., F. Sun, and S. Song, *Opt. Express*, Vol. 21, No. 13, 15896–15903, 2013.
15. Johnson, P. B. and R. W. Christy, *Phys. Rev. B*, Vol. 6, No. 12, 4370–4379, 1972.
16. Koppens, F. H. L., D. E. Chang, and F. J. G. de Abajo, *Nano. Lett.*, Vol. 11, No. 8, 3370–3377, 2011.
17. Gusynin, V. P., S. G. Sharapov, and J. P. Carbotte, *Phys. Rev. B*, Vol. 75, 165407, 2007.
18. Mak, K. F., M. Y. Sfeir, Y. Wu, C. H. Lui, J. A. Misewich, and T. F. Heinz, *Phys. Rev. Lett.*, Vol. 101, 196405, 2008.
19. Smith, D. R., S. Schultz, P. Markos, and C. M. Soukoulis, *Phys. Rev. B*, Vol. 65, No. 19, 195104, 2002.
20. Song, S. C., Q. Chen, L. Jin, and F. H. Sun, *Nanoscale*, Vol. 5, No. 20, 9615–9619, 2013.